Title
Model Simulation of the Influence of Global SST Anomalies on Sahel Rainfall

Journal
Monthly Weather Review, 126(11)

ISSN
0027-0644

Authors
Xue, Yongkang
Shukla, Jagadish

Publication Date
1998-11-01

DOI
10.1175/1520-0493(1998)126<2782:msotio>2.0.co;2

Peer reviewed

Model Simulation of the Influence of Global SST Anomalies on Sahel Rainfall

YONGKANG XUE* AND JAGADISH SHUKLA

Center for Ocean–Land–Atmosphere Studies, Calverton, Maryland

(Manuscript received 21 March 1997, in final form 7 November 1997)

ABSTRACT

A general circulation model sensitivity study was carried out to investigate the influence of global sea surface temperature (SST) on Sahel rainfall. This study was inspired by the impressive model simulations of Sahel rainfall reported by Folland et al. and Rowell et al. The model was integrated from June through September with three different atmospheric initial conditions and four years (1950, 1958, 1983, and 1984) of SST. In three out of four cases (1950, 1983, 1984), the area-averaged simulated rainfall anomaly was consistent with the observations. However, the model's internal variability was rather large. The simulated anomalies had relatively larger sensitivity to the initial conditions in this study than those in a desertification study performed previously by the authors. This model failed to simulate the rainfall anomaly for 1958. Additional model experiments are needed to establish the role of SST variation in determining the Sahel rainfall variation.

1. Introduction

A large amount of evidence based on observational and modeling studies has established a strong relationship between the changes in the slowly varying boundary conditions at the earth's surface [e.g., sea surface temperature (SST) and land surface conditions] and changes in atmospheric circulation and rainfall. The underlying mechanisms responsible for such a relationship have been presented and reviewed in several papers (viz. Charney and Shukla 1981; Shukla 1984; and numerous others for SST; Charney et al. 1977; Shukla and Mintz 1982; Xue et al. 1990; Dirmeyer and Shukla 1993; Xue 1997, and others for land surface conditions). Since the dynamical flow instabilities are relatively weaker in the Tropics (compared to midlatitudes), the boundary-forced changes in circulation and rainfall dominate at seasonal and interannual timescales. The manner in which a given boundary anomaly influences the circulation and rainfall for any particular region naturally depends upon the structure of the large-scale flow for that region and the presence or absence of other quasi-stationary forcings (viz. orography and mean heat sources and sinks in that region).

The relationship between SST and seasonal to interannual rainfall variations in the Sahel region has long been an important scientific subject under investigation. The first comprehensive observational evidence for a possible relationship between the Atlantic SST anomalies and the Sahel rainfall anomalies was presented by Lamb (1978a,b). Lamb showed a relationship between displacements of SST patterns and rainfall patterns. This result was further confirmed, and extended to explain long-term changes, by several subsequent studies (Hastenrath 1984, 1990; Druyan 1991; Lamb and Peppler 1991).

Several other observational and modeling studies have suggested that the global SST anomalies also play an important role in producing rainfall anomalies over the Sahel and the adjoining regions (Folland et al. 1986; Palmer 1986; Folland et al. 1991; Palmer et al. 1992; Rowell et al. 1995). Folland et al. (1991) found that the relatively modest variations observed in the large-scale patterns of SST have had a substantial impact on the variations of Sahel rainfall. Tropical oceans, on the whole, have considerably more influence than extratropical oceans. They also found that warmer SST in the Southern Hemisphere relative to that in the Northern Hemisphere has been associated with Sahel drought.

The present study was motivated by the impressive results presented by Folland et al. (1991) and Rowell et al. (1995). Considering the large sensitivity of tropical rainfall to changes in SST, it is quite reasonable to expect that a good dynamical model can successfully simulate the observed SST–rainfall relationship. However, we were intrigued by the degree of success (near-perfect correlation between the sign of the observed and model simulated rainfall anomalies, and excellent simulation of the annual cycle and the seasonal mean rainfall in

* Current affiliation: Department of Geography, University of Maryland, College Park, Maryland.

Corresponding author address: Dr. Yongkang Xue, Department of Geography, University of Maryland, College Park, MD 20742.
E-mail: yxue@geog.umd.edu

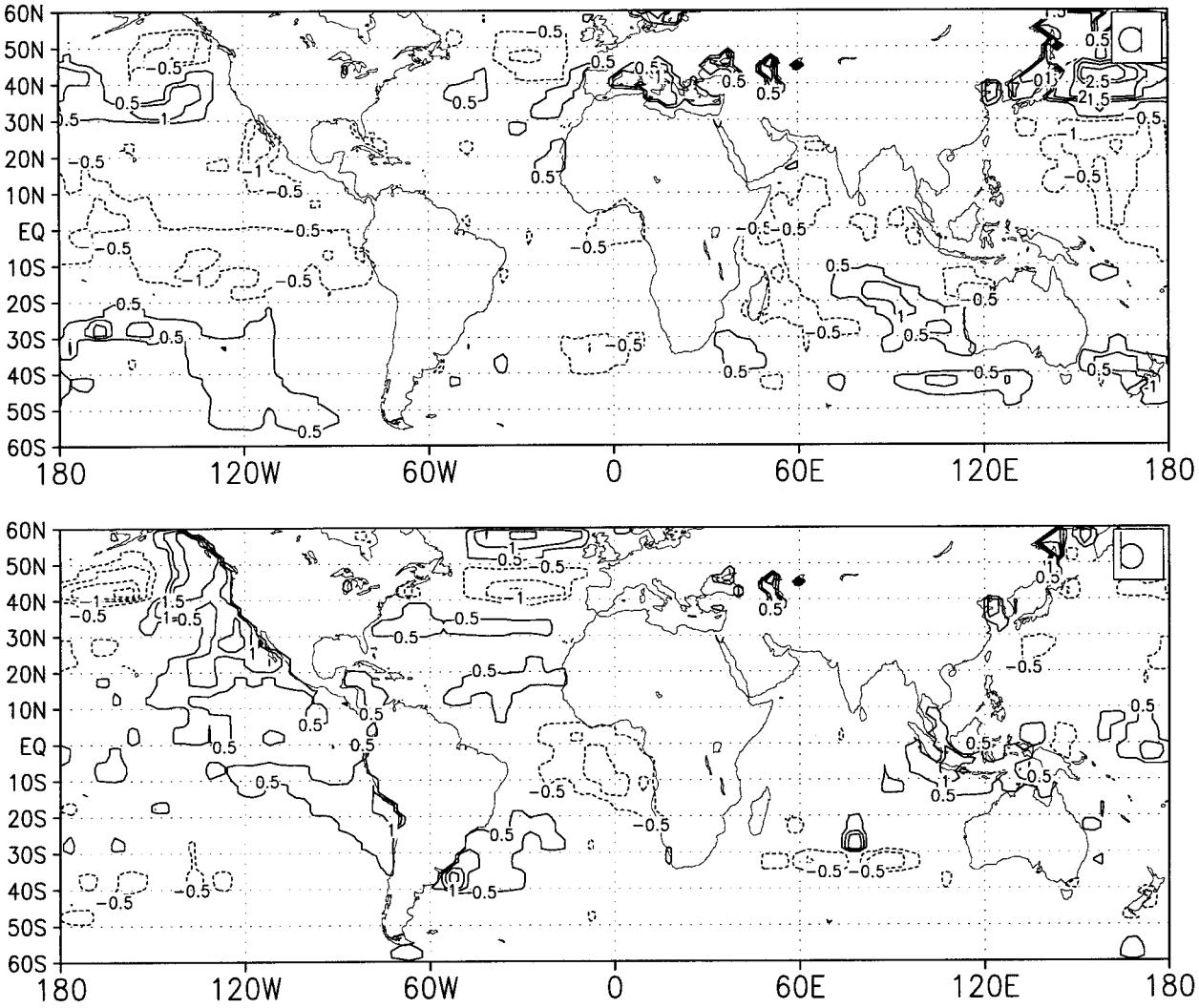

FIG. 1. Sea surface temperature anomalies for (a) 1950, (b) 1958, (c) 1983, and (d) 1984. Units: K. The climatological period, from which anomalies were calculated, is from 1951 to 1980.

the Sahel region) for 10 selected years. In the remainder of this paper we will refer to the paper by Rowell et al. (1995) as RFMW. Our primary motivation was to investigate the reproducibility of these results by another global model. We would like to clarify at the outset that even if no other model can reproduce the results of RFMW (Sud and Lau 1996), it, by no means, questions the validity of these results. We fully recognize how complex a global climate model is, and it is highly unlikely that a climate model will produce 10 highly successful simulations just by chance.

2. Model and experimental design

The Center for Ocean–Land–Atmosphere (COLA) general circulation model (GCM) used in the present study is exactly the same as the one used by Xue and Shukla (1993, 1996) to investigate the effects of changes in the land surface conditions on sub-Saharan rainfall. This will make it possible to compare the relative impacts of changes in SST and land surface conditions.

The COLA GCM is based on a modified version of the National Centers for Environmental Prediction (formerly the National Meteorological Center) global spectral model with rhomboidal truncation at zonal wavenumber 40 (Kinter et al. 1988; Sato et al. 1989). The prognostic computations are carried out in the spectral domain and the physical processes are computed on a Gaussian grid (with approximately 1.8° latitude by 2.8° longitude resolution). The model is discretized into 18 vertical layers. A modified Kuo scheme is used for cumulus convection (Kuo 1965). An interactive cloud scheme, similar to the one developed by Slingo (1987), was incorporated into the GCM for the radiation calculations (Hou 1990).

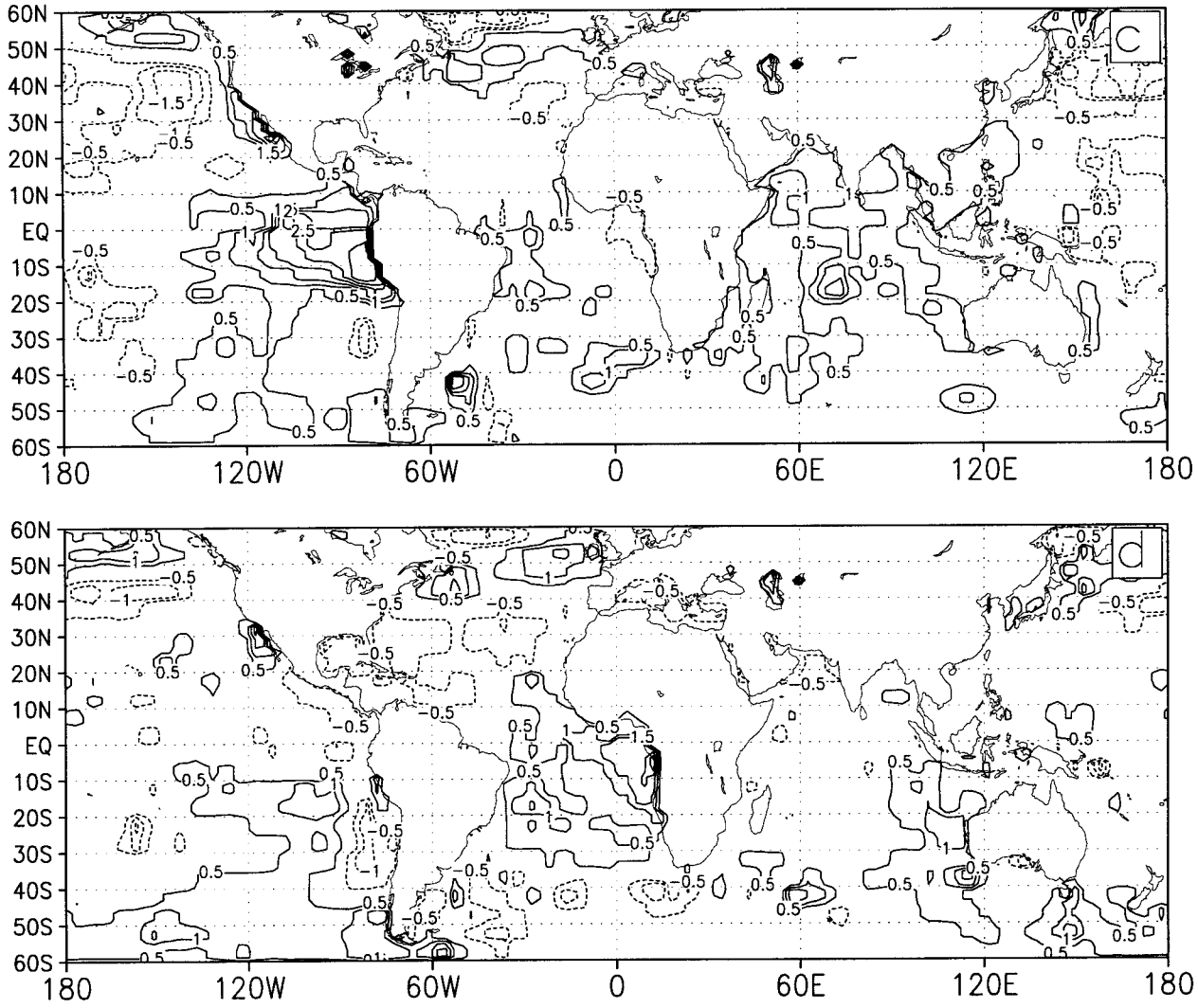

FIG. 1. (*Continued*)

The purpose of this study is to investigate the effects of the global SST anomalies on the sub-Saharan rainfall. The COLA GCM was first integrated with climatological SST for 4 months starting from three initial atmospheric conditions for 1–3 June 1988. The averages for these three integrations were referred to as the CONTROL integration. These three seasonal integrations were repeated four more times using the observed global SST for 1950, 1958, 1983, and 1984. These are 4 of the 10 years chosen by RFMW and the same 4 years used by Folland et al. (1991). The averages of three integrations using four different SSTs will be referred to as SST50, SST58, SST83, and SST84, respectively. The land surface conditions (vegetation, soil wetness, etc.) were the same in all the integrations. The monthly mean global SST data (Bottomley et al. 1990), which are the same as those used by Folland et al. (1991) in their simulations, were kindly provided by the U.K. Meteorological Office. During the integration, the model interpolates daily values of SST at each grid point. The differences in results of this study and that of RFMW can be largely attributed to the differences in the two models.

3. Observed SST anomalies

Figure 1 shows the observed July, August, September (JAS) SST anomalies for each of the four years. Out of these four years, 1983 and 1984 represent the two dry years for Sahel and 1950 and 1958 represent two wet years.

In 1950 there are no significant SST anomalies in the tropical Atlantic (only a mild dipole pattern). The equatorial Pacific is colder than normal and the northern Pacific Ocean is warmer than normal. Very pronounced SST anomalies are seen in the southern Indian Ocean.

In 1958 there is a well-defined SST anomaly dipole pattern in the tropical Atlantic with warmer than average SSTs to the north and colder than average to the south of the equator. The eastern tropical Pacific Ocean is generally warmer than normal and there are no significant SST anomalies in the Indian Ocean. The SST anomaly map for 1983 is dominated by large positive SST anomalies in the eastern topical Pacific associated with one of the major El Niño events of this century. The SST in the northern Pacific Ocean is colder than normal. The southern Atlantic and the Indian Ocean are generally warmer than normal. In 1984 there is also an SST anomaly dipole pattern in the Atlantic Ocean similar to that in 1958 except that it is stronger and of opposite polarity, showing positive SST anomalies to the south of the equator. The eastern equatorial Pacific SST anomalies are negative near most of the coastal areas.

The main purpose of showing actual SST anomalies is to point out that, with the exception of the 1983 warm event in the Pacific, the tropical SST anomalies in general, and over the Atlantic in particular, are rather modest in amplitude. To the extent that they can still produce a rather significant change in precipitation over the Sahel region is indeed very impressive.

4. Results

a. Mean rainfall

Figure 2b shows the JAS rainfall for the mean of SST50, SST58, SST83, and SST84. The observed African rainfall is from Nicholson (1993). In the simulations, the rainfall in the sub-Saharan region was greater than the observed and the extent of the intertropical convergence zone was greater than the observation (Fig. 2a). These results are consistent with the seasonal mean rainfall simulated in Xue and Shukla (1993) and will not be further elaborated here. Following RFMW, we have defined a region between 13°N and 17°N and 15°W and 40°E for averaging rainfall for more detailed comparison. For convenience, hereafter, we will refer to this region as Sahel. The average Sahel rainfalls (in the units of mm day^{-1}) for the CONTROL integration and for the four observed SST integrations (SST50, SST58, SST83, and SST84) are 5.81 and (6.29, 5.57, 4.94, 5.17), respectively. The corresponding long-term observed climatological rainfall, which is the mean of all available rainfall data, and the observed rainfall for the years (1950, 1958, 1983, 1984) are 3.48 and (5.03, 4.33, 2.40, 1.83), respectively. It should be pointed out that the simulated mean rainfall in RFMW was much closer to the observed rainfall especially for the Sahel region. However, as shown in Fig. 2, overall, the major rainfall patterns are fairly well simulated in the COLA GCM.

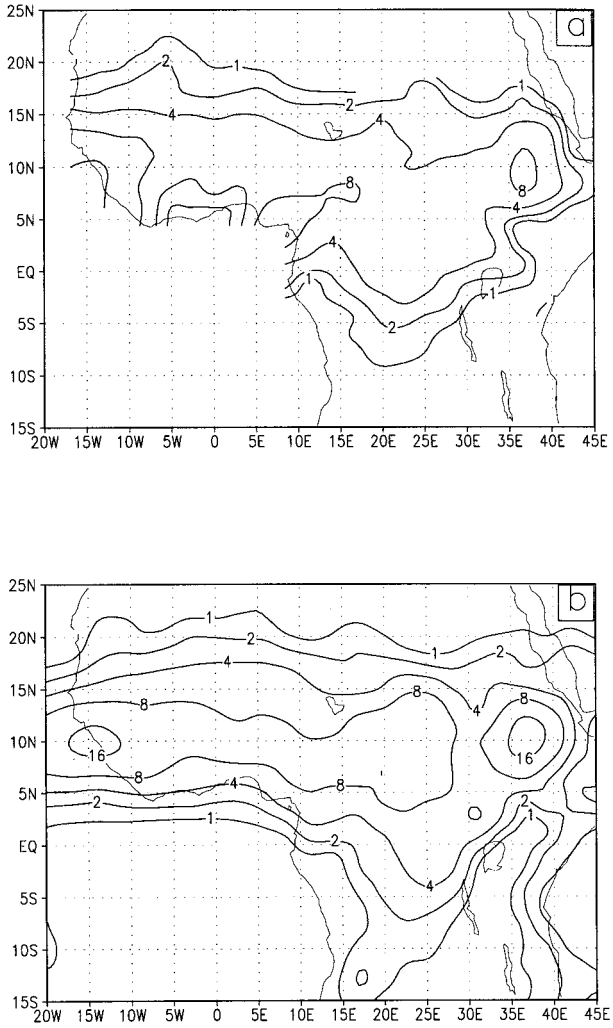

FIG. 2. (a) Observed JAS rainfall for the mean of 1950, 1958, 1983, and 1984; (b) simulated JAS rainfall for the mean of SST50, SST58, SST83, and SST84. Units: mm day^{-1}.

b. Rainfall anomalies

Figures 3, 4, 5, and 6 show the model-simulated and observed rainfall anomalies for each of the years 1950, 1958, 1983, 1984, respectively. Each figure has four panels. The first three panels (a, b, c) show the model-simulated rainfall anomaly for three different model integrations starting from slightly different initial conditions on 1, 2, and 3 June of each year. Thus, the first three panels of simulated JAS rainfall anomaly are for the same SST anomaly. The fourth panel (d) shows the observed JAS rainfall anomaly for that year. The model-simulated rainfall anomaly is calculated by subtracting the CONTROL integration from the observed SST integration. For example, (SST501 minus CONTROL1) and (SST502 minus CONTROL2) gives the model-simulated rainfall anomaly for 1950 with 1 June and 2 June initial conditions, respectively. The observed rainfall

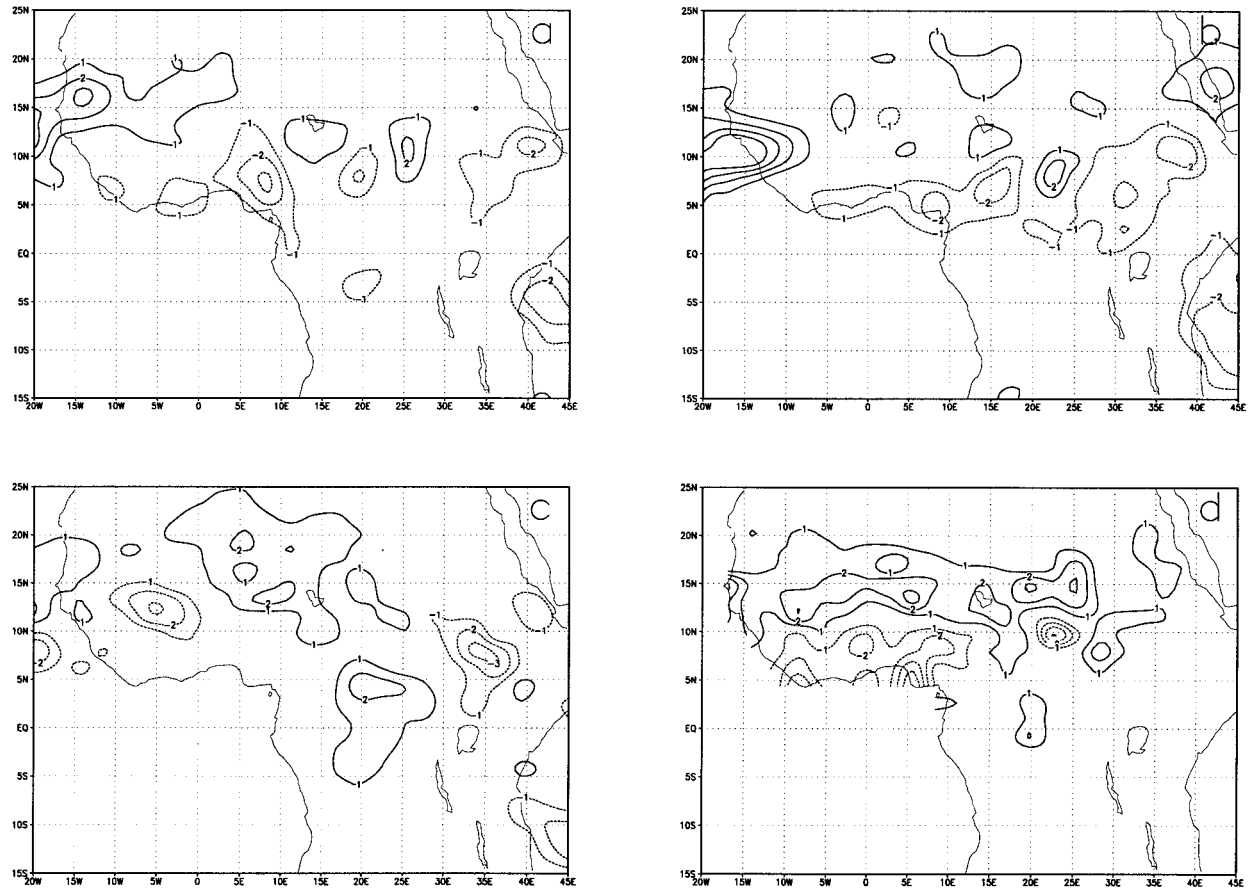

FIG. 3. Simulated JAS rainfall difference between (a) SST501 and CONTROL1, (b) SST502 and CONTROL2, and (c) SST503 and CONTROL3; (d) observed JAS rainfall anomaly for 1950. Units: mm day^{-1}.

anomaly was obtained from all the available stations for that year.

The most noteworthy features of these figures are large differences among three integrations with slightly different initial conditions for the same SST anomaly. The only exception is 1983 (Fig. 5), for which there is considerable reproducibility among the three model simulations for three different initial conditions. However, even for 1983 there are large errors in simulated rainfall anomalies for specific regions. For example, between 5°–10°N and 5°–15°W the model shows the largest positive rainfall anomalies over that region where the observations had the largest negative anomalies. Simulated rainfall anomalies for 1958 (Fig. 4) are not only quite different from each other for the three initial conditions, but they have little similarity to the observed rainfall anomaly (Fig. 4d). This is especially puzzling because 1958 SST anomalies show a well-defined dipole pattern in the tropical Atlantic.

The results in this study reveal a high sensitivity of the simulated anomalies to initial conditions, which is quite different from our land processes experiments (Xue and Shukla 1993, 1996; Xue 1997). In land studies, the changes in land surface conditions were rather dramatic. The strong local anomaly forcing produced stable anomaly rainfall patterns with less sensitivity to the initial conditions. Because the SST anomaly affects Sahel mainly through change in the atmosphere circulation (see more detailed discussion in next section), the internal variability became much higher in model simulations.

Whereas the individual rainfall anomaly maps look disorganized, a spatial averaging of rainfall anomalies over the Sahel region gives a very different picture. Figure 7 shows the model-simulated and observed rainfall anomalies averaged over the Sahel region defined earlier. The three bars for each year correspond to the three model simulations with three different initial conditions. The sign of the rainfall anomalies is correctly simulated in three out of four years. However, the amplitude of the simulated rainfall anomaly is only comparable to the observations in 1983. For 1958, the simulated rainfall anomalies are negative in two cases while the observed anomaly is positive. For 1950 and 1984, the simulated rainfall anomaly is only about one-third of the observed rainfall anomaly.

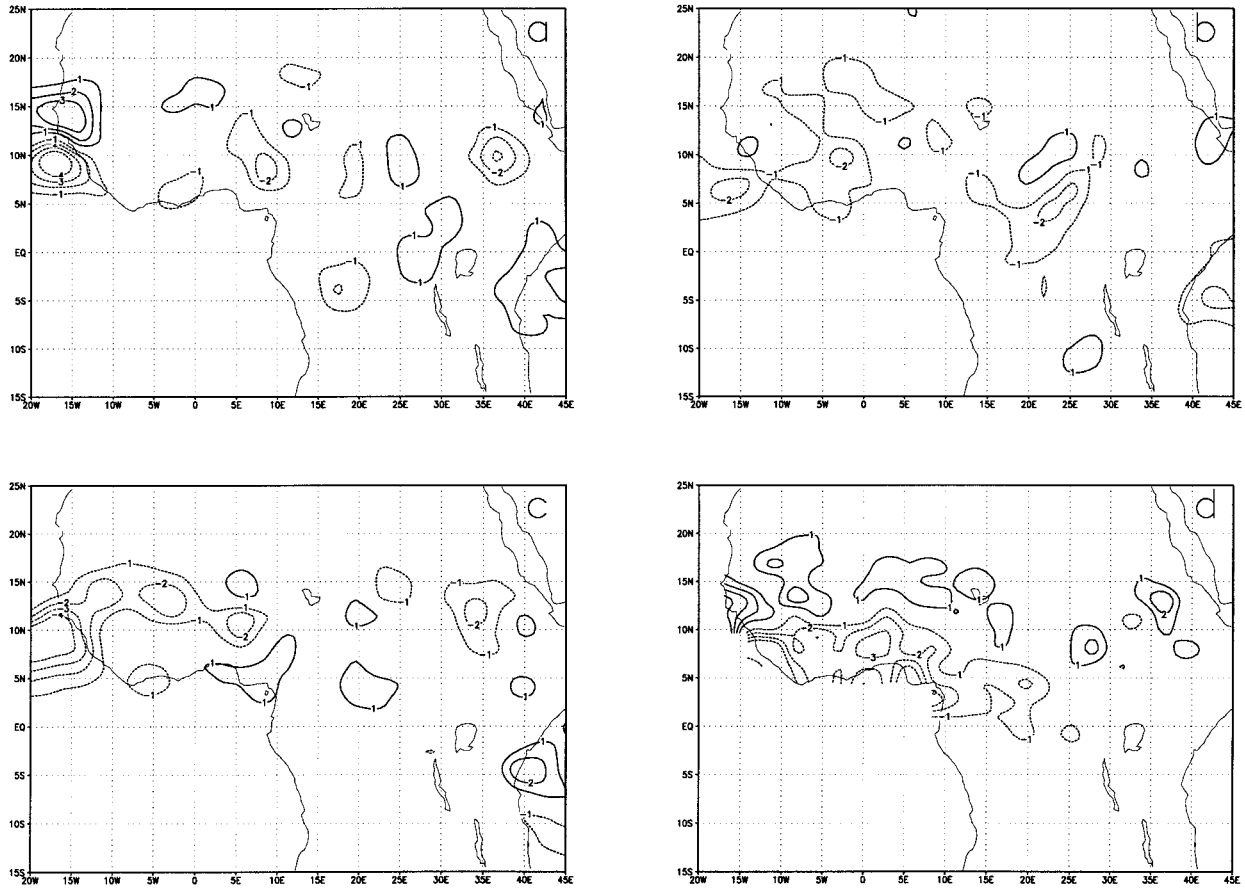

FIG. 4. Simulated JAS rainfall difference between (a) SST581 and CONTROL1, (b) SST582 and CONTROL2, and (c) SST583 and CONTROL3; (d) observed JAS rainfall anomaly for 1958. Units: mm day^{-1}.

In order to test the statistical significance of results, long-term integrations may be necessary. However, testing statistical significance was not our primary goal. In this study, we used several different initial conditions with each SST to reduce model internal variability. We also carried out Student's t-tests for each year. Three CONTROL and three observed SST integrations for three initial conditions for each year were used to calculate t values. It was found (not shown) that the simulated rainfall anomalies for all years are not statistically significant even at the 90% significant level. However, despite the failure in simulating the 1958 anomaly, a Student's t-test for the JAS rainfall differences between the mean of SST83 and SST84 and the mean of SST50 and SST58 shows that the rainfall differences between them are significant at a 90% level over the central Sahel area (for the negative anomaly), and the area near the Gulf of Guinea and part of eastern Africa (for the positive anomaly; Fig. 8). It should also be pointed out that the significance of the positive anomaly near the Gulf of Guinea is questionable. As shown in Fig. 4, there was no positive anomaly near the Gulf of Guinea in 1983. The positive anomaly in Fig. 8a was mainly caused by the 1984 rainfall anomaly. Although the model correctly simulates the 1984 positive anomaly, the simulated 1983 positive anomaly near the Gulf of Guinea is not found in the observations. However, this error actually enhances the significance of the positive anomaly in Fig. 8b.

c. *Moisture flux convergence*

Precipitation over a region is linked to the atmospheric circulation through the regional convergence of atmospheric moisture:

$$\Delta S = E - g^{-1} \int \nabla(P_S q V)\, d\sigma - P,$$

where S is the change in atmospheric moisture content, E is evapotranspiration, P_S is surface pressure, q is specific humidity, V is the horizontal wind velocity, σ is the model vertical coordinate system, and P is precipitation. The rainfall anomalies in this study are closely associated with the variations in moisture flux convergence (MFC). Figures 9a–d are the differences of MFC

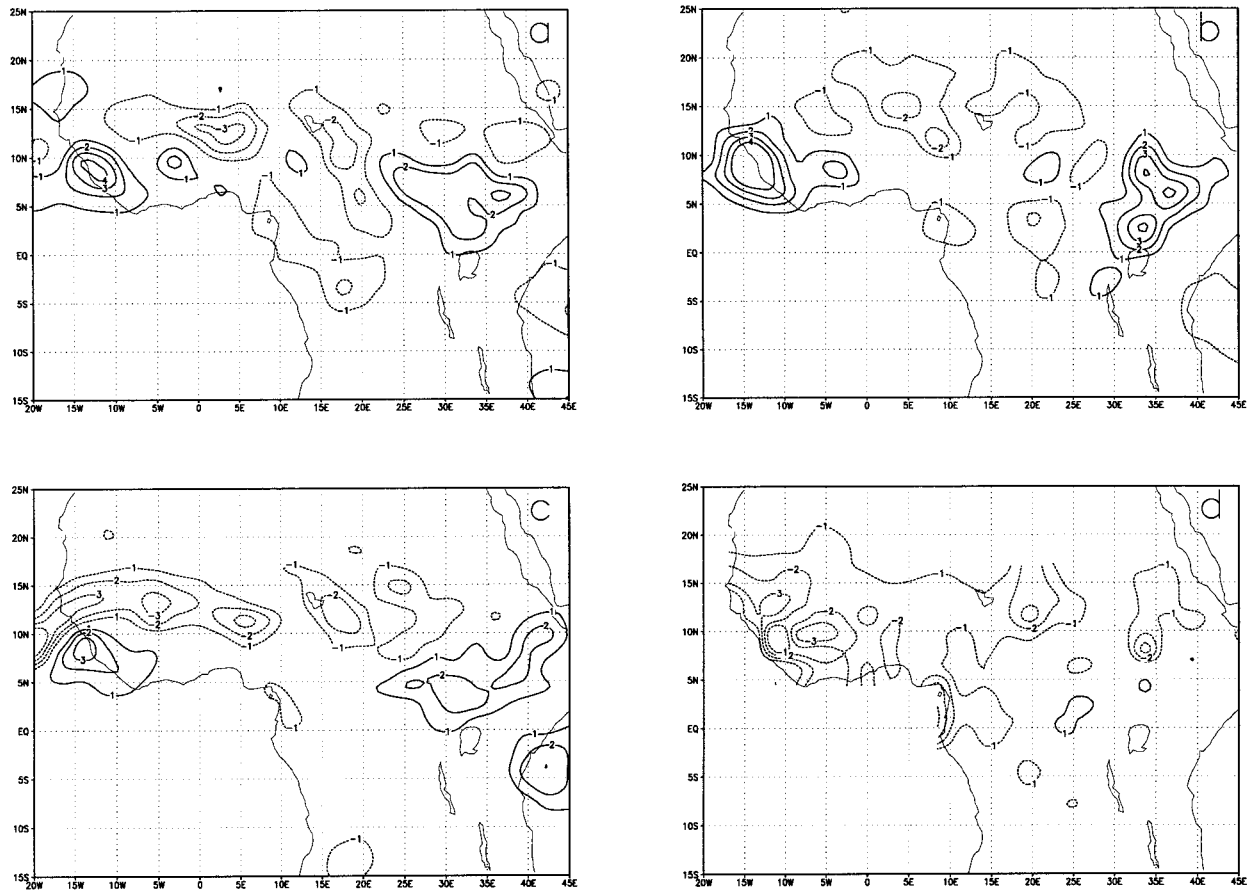

FIG. 5. Simulated JAS rainfall difference between (a) SST831 and CONTROL1, (b) SST832 and CONTROL2, and (c) SST833 and CONTROL3; (d) observed JAS rainfall anomaly for 1983. Units: mm day^{-1}.

averaged over 15°W and 40°E between SST50 and CONTROL, SST58 and CONTROL, SST83 and CONTROL, and SST84 and CONTROL, respectively. There are strong gradients between 10° and 15°N in the low and middle atmosphere. All four cases have enhanced MFC (or reduced moisture flux divergence, MFD) below 850 mb near 15°N. This enhancement extends to 700 mb in SST50, which is consistent with the rainfall increase in SST50. In both SST83 and SST84, the MFC is reduced (or MFD is increased) above 850 mb. The vertically integrated MFC over the Sahel region is reduced by 0.72 mm day^{-1} for SST83 and 0.41 mm day^{-1} for SST84. Rowell et al. (1992) found that their simulated Sahel precipitation was primarily associated with changes in the midlevel convergence of moisture. The low-level moisture accumulation was even larger in 1983, which is quite consistent with our results. The changes above 850 mb in SST58 are similar to SST83 and SST84, but weak. The vertically integrated MFC has no change.

In SST50 and SST58, a reduced MFC near the surface is located to the south of the area associated with enhanced MFC. The rainfall there is reduced (Figs. 3 and 4). In SST83 and SST84, the enhanced MFC area near the surface expands to the south, and to the middle troposphere. These changes are consistent with positive rainfall anomalies there in the model simulations. The subsidence at midtroposphere above the Sahel region increases in SST83 and SST 84 and decreases in SST50 (not shown), which is consistent with the MFC changes. In SST58, the rising motion increases over the Sahel region (not shown). But this change does not lead to a corresponding change in rainfall and MFC. The differences in P, E, and vertically integrated MFC over the Sahel region between the mean of SST83 and SST84, and the mean of SST50 and SST58, are -0.88 mm day^{-1}, -0.22 mm day^{-1}, and -0.72 mm day^{-1}, respectively. Changes in P are dominated by changes in MFC. Evaporation and cloud cover, as well as soil moisture, have only small changes (not shown), which are quite different from our results in desertification (Xue and Shukla 1993; Xue 1997). However, this feature may help us to understand one of Rowell et al.'s (1995) results, in which an interactive soil scheme made very little difference compared with specified soil moisture. The limited cloud cover change may also be a cause of

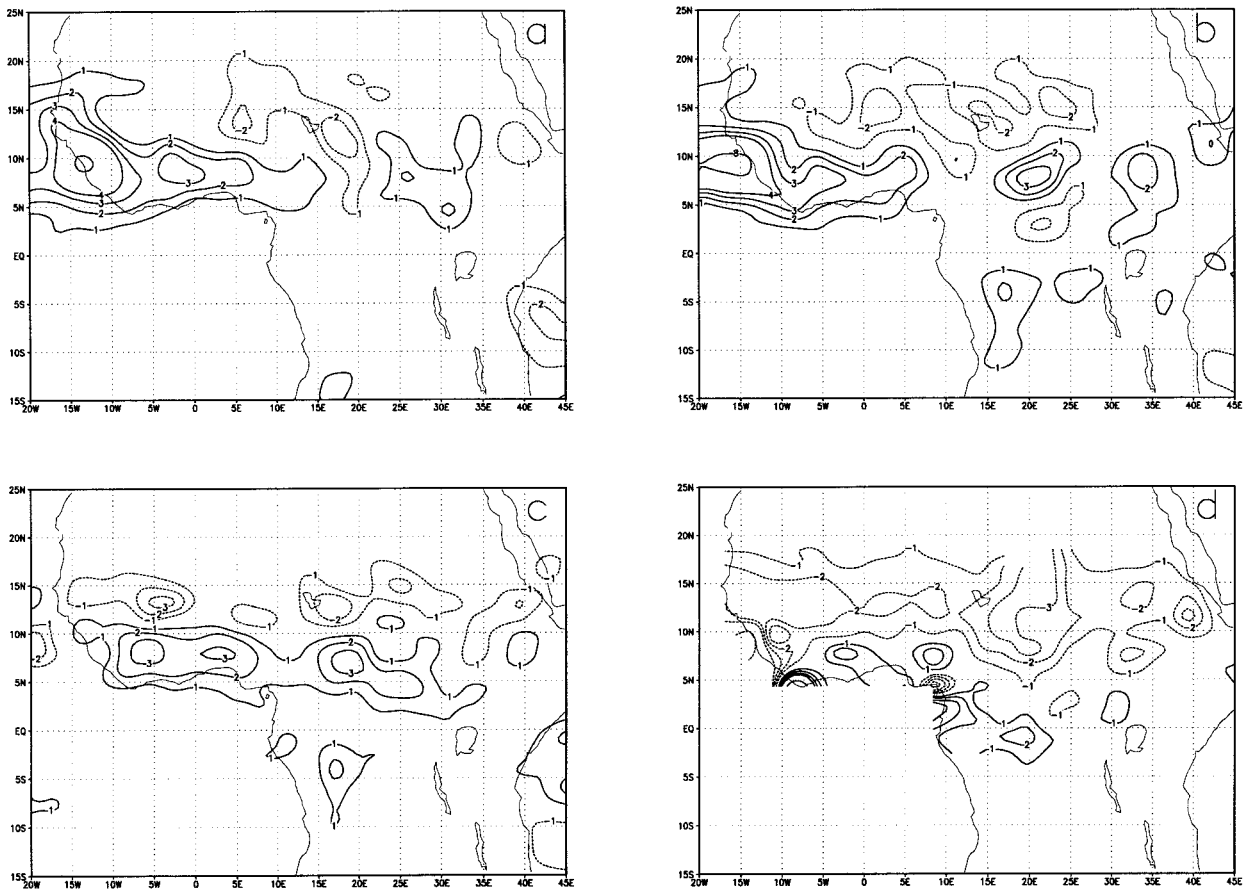

FIG. 6. Simulated JAS rainfall difference between (a) SST841 and CONTROL1, (b) SST842 and CONTROL2, and (c) SST843 and CONTROL3; (d) observed JAS rainfall anomaly for 1984. Units: mm day^{-1}.

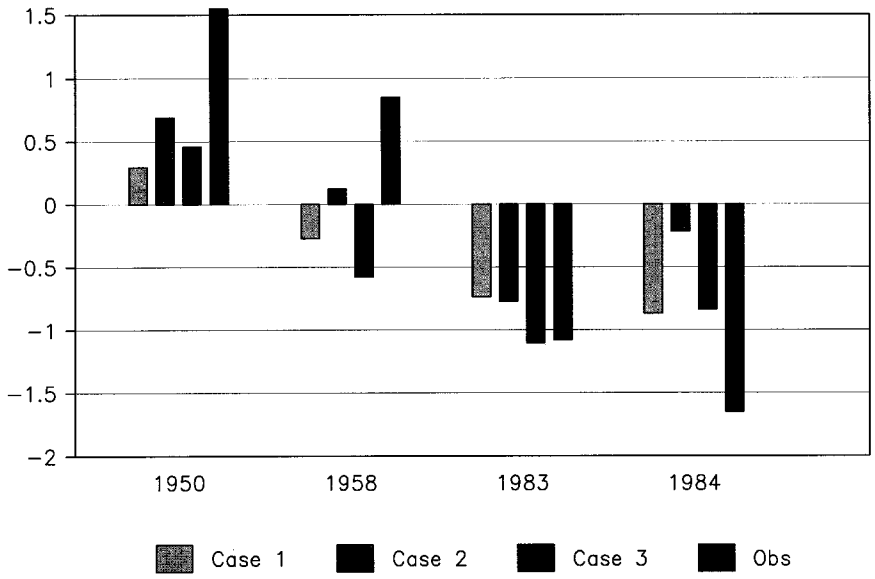

FIG. 7. Simulated rainfall anomaly for each case and climatological rainfall for each year over the test area. Units: mm day^{-1}.

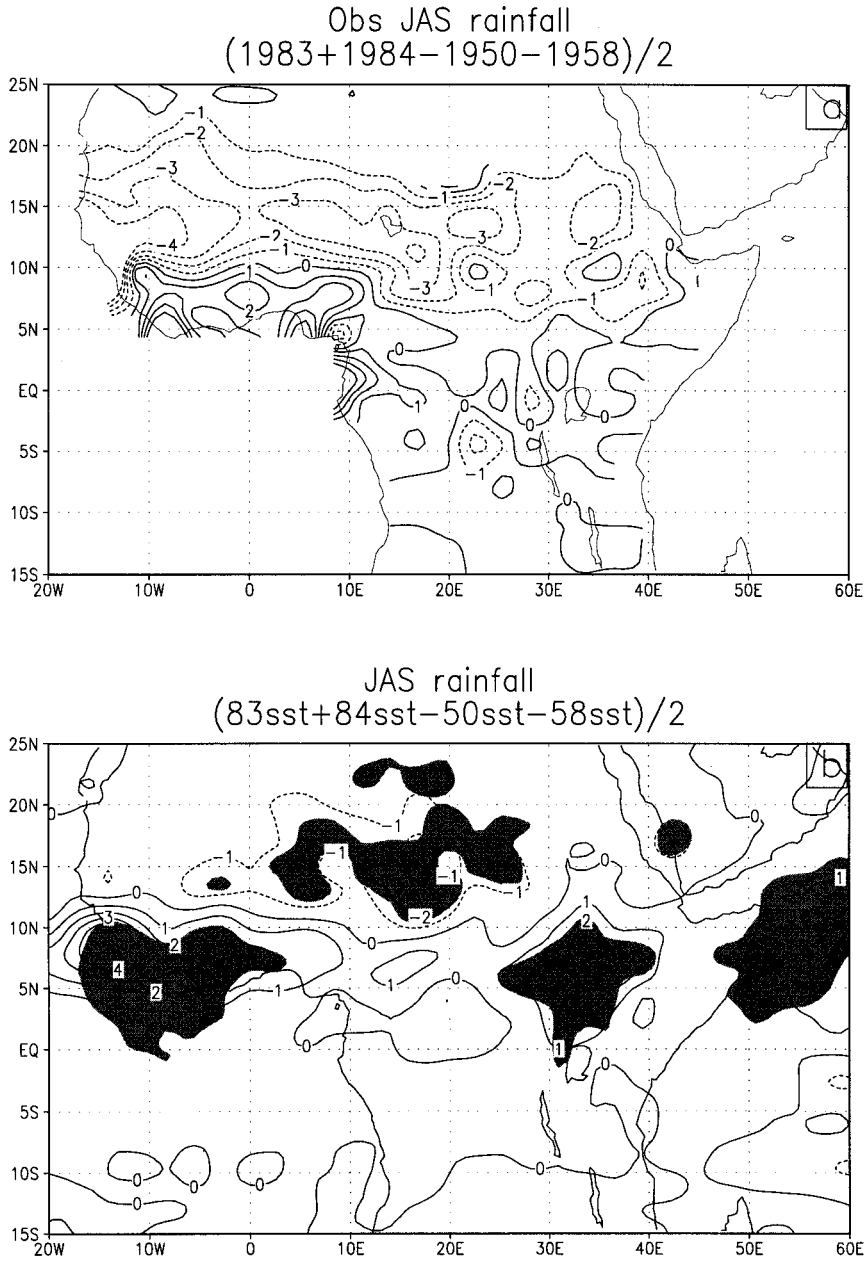

FIG. 8. (a) Observed JAS rainfall difference between two dry years (1983 and 1984) and two wet years (1950 and 1958); (b) simulated JAS rainfall difference between the mean of SST83 and SST84 and the mean of SST50 and SST58. The area in which the difference has more than 90% significant level is shaded. Units: mm day^{-1}.

overall reduced sensitivity in our SST study. But we do not know if this is caused by the cloud scheme or by atmospheric circulation simulation.

5. Discussion and summary

This study was inspired by the successful model simulations of Sahel rainfall using observed SSTs (Folland et al. 1991; Rowell et al. 1995) and was intended to investigate the reproducibility of these results by another GCM, the COLA GCM, which has also been used for a number of Sahel studies.

The results from this study generally support the results from other studies that the SST has identifiable impact on the Sahel rainfall. In three out of four runs (SST50, SST83, SST84), the simulated rainfall anomaly averaged over Sahel region is consistent with the observations, but with large internal variability. The simulated anomalies had rel-

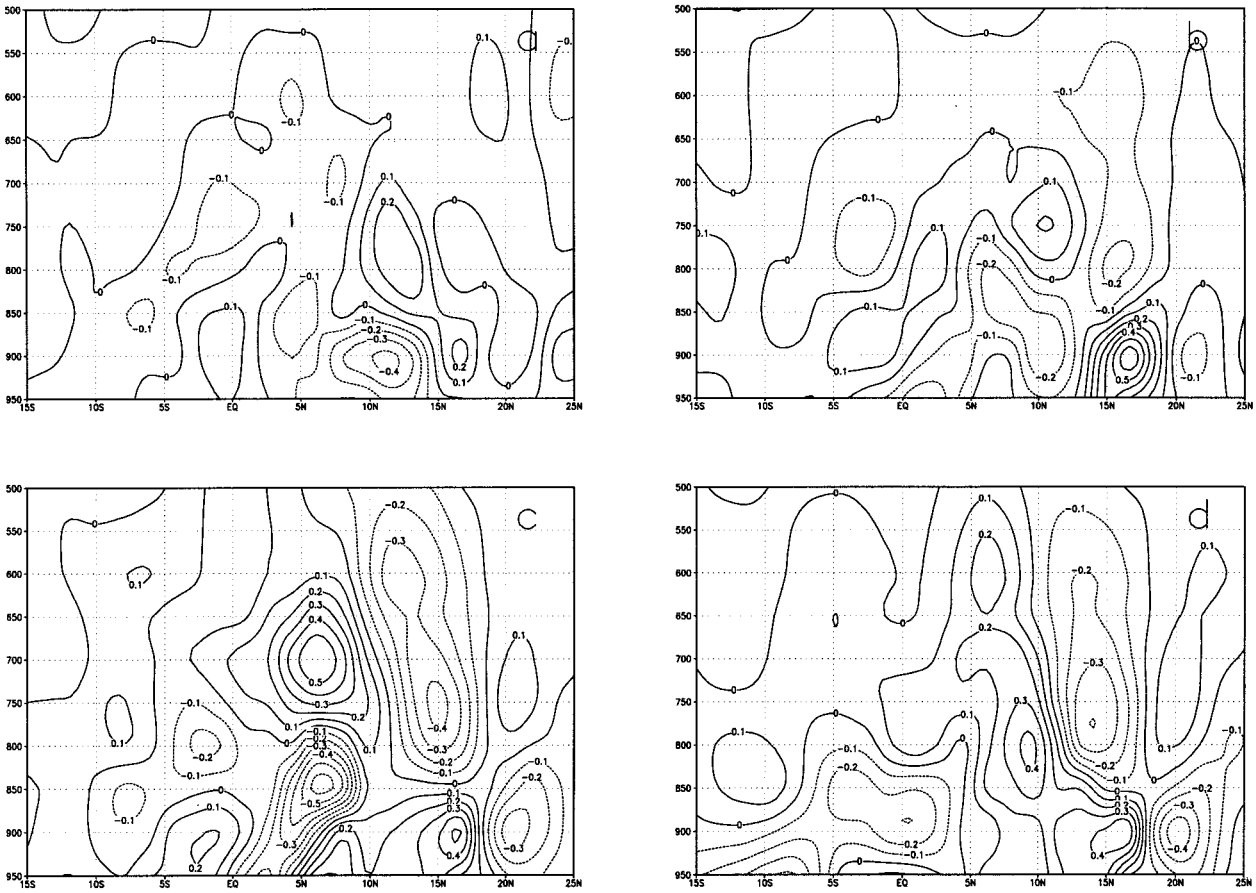

FIG. 9. JAS moisture flux convergence averaged over 15°W and 40°E for (a) SST50 minus CONTROL, (b) SST58 minus CONTROL, (c) SST83 minus CONTROL, and (d) SST84 minus CONTROL. Units: mm day^{-1}.

atively larger sensitivity to the initial conditions in this study than those in our desertification study (Xue and Shukla 1993). The changes in simulated seasonal mean Sahel rainfall is consistent with the changes in MFC at middle-atmospheric levels as also discovered by Rowell et al. (1992). However, the patterns of simulated rainfall anomaly are quite different from observations. We summarize below the differences between the results found here and earlier studies.

First, comparing the results from this study and the results from Folland et al. (1991), we find that the simulated SST impact on the Sahel rainfall is model dependent. For example, the simulation of 1958 is quite different in the COLA GCM and the U.K. Meteorological Office model.

Second, the simulated rainfall anomalies in this study are smaller than observed ones. In one case (SST58), the model cannot produce the observed rainfall anomaly pattern at all. The results from the desertification experiments (Xue and Shukla 1993; Xue 1997) showed that despite the dramatic changes in prescribed land surface conditions in the desertification experiment, the simulated rainfall anomaly was still smaller than observations. In the COLA GCM, neither SST nor land anomaly forcing alone would produce the observed rainfall anomalies. It is likely that both SST and land surface anomalies play a role in simulation of Sahel rainfall.

Acknowledgments. This research was supported by the National Science Foundation through Grants ATM-93-41271 and EAR-94-05431. We are thankful to the U.K. Meteorological Office for providing the SST data for this study. We would also like to thank F. J. Zeng for assistance in preparation of this paper.

REFERENCES

Bottomley, M., C. K. Folland, J. Hsiung, R. E. Newell, and D. E. Parker, 1990: *Global Ocean Surface Temperature Atlas 'GOSTA.'* Her Majesty's Stationery Office, 20 + iv pp. and 313 plates.

Charney, J. G., and J. Shukla, 1981: Predictability of monsoon. *Monsoon Dynamics*, J. Lighthill and R. P. Pearce, Eds., Cambridge University Press.

——, W. K. Quirk, S.-H. Chow, and J. Kornfield, 1977: A comparative study of the effects of albedo change on drought in semi-arid regions. *J. Atmos. Sci.*, **34,** 1366–1385.

Dirmeyer, P. A., and J. Shukla, 1993: Observational and modeling studies of the influence of soil moisture anomalies on atmo-

spheric circulation. *Prediction of Interannual Climate Variations,* J. Shukla, Ed., NATO Series I, Vol. 6, Springer-Verlag, 1–23.

Druyan, L. M., 1991: The sensitivity of sub-Saharan precipitation to Atlantic SST. *Climate Change,* **18,** 17–36.

Folland, C. K., T. N. Palmer, and D. E. Parker, 1986: Sahel rainfall and worldwide sea temperatures, 1901–85. *Nature,* **320,** 602–607.

——, J. Owen, M. N. Ward, and A. Colman, 1991: Prediction of seasonal rainfall in the Sahel region using empirical and dynamical methods. *J. Forecasting,* **1,** 21–56.

Hastenrath, S., 1984: International variability and annual cycle: Mechanisms of circulation and climate in the tropical Atlantic sector. *Mon. Wea. Rev.,* **112,** 1097–1107.

——, 1990: Decadal-scale changes of the circulation in the tropical Atlantic sector associated with Sahel drought. *Int. J. Climatol.,* **10,** 459–472.

Hou, Y.-T., 1990: Cloud-radiation-dynamics interaction. Ph.D. dissertation, University of Maryland, 209 pp. [Available from University of Maryland at College Park, College Park, MD 20742.]

Kinter, J. L., III, J. Shukla, L. Marx, and E. K. Schneider, 1988: A simulation of the winter and summer circulations with the NMC global spectral model. *J. Atmos. Sci.,* **45,** 2486–2522.

Kuo, H. L., 1965: On formation and intensification of tropical cyclones through latent heat release by cumulus convection. *J. Atmos. Sci.,* **22,** 40–63.

Lamb, P. J., 1978a: Large-scale tropical Atlantic surface circulation patterns associated with sub-Saharan weather anomalies. *Tellus,* **30,** 240–251.

——, 1978b: Case studies of tropical Atlantic surface circulation patterns during recent sub-Saharan weather anomalies: 1967 and 1968. *Mon. Wea. Rev.,* **106,** 482–491.

——, and R. A. Peppler, 1991: West Africa. *Teleconnections Linking Worldwide Climate Anomalies,* M. Glantz, R. W. Katz, and N. Nicholls, Eds., Cambridge University Press, 121–189.

Nicholson, S. E., 1993: An overview of African rainfall fluctuations of the last decade. *J. Climate,* **6,** 1463–1466.

Palmer, T. N., 1986: Influence of the Atlantic, Pacific and Indian Oceans on Sahel rainfall. *Nature,* **322,** 251–253.

——, C. Brankovic, P. Viterbo, and M. J. Miller, 1992: Modeling interannual variations of summer monsoons. *J. Climate,* **5,** 399–417.

Rowell, D. P., C. K. Folland, K. Maskell, J. A. Owen, and M. N. Ward, 1992: Modeling the influence of global sea surface temperatures on the variability and predictability of seasonal Sahel rainfall. *Geophys. Res. Lett.,* **19,** 905–908.

——, ——, ——, and M. N. Ward, 1995: Variability of summer rainfall over tropical north Africa (1906–92): Observation and modeling. *Quart. J. Roy. Meteor. Soc.,* **121,** 669–704.

Sato, N., P. J. Sellers, D. A. Randall, E. K. Schneider, J. Shukla, J. L. Kinter III, Y.-T. Hou, and E. Albertazzi, 1989: Effects of implementing the simple biosphere model in a general circulation model. *J. Atmos. Sci.,* **46,** 2757–2782.

Shukla, J., 1984: Predictability of time averages: II. The influence of boundary forcings. *Problems and Prospects in Long and Medium Range Forecasting,* D. M. Burridge and E. Kallen, Eds., Springer, 109–206.

——, and Y. Mintz, 1982: Influence of land-surface evapotranspiration on the earth's climate. *Science,* **215,** 1498–1501.

Slingo, J. M., 1987: The development and verification of a cloud prediction scheme for the ECMWF model. *Quart. J. Roy. Meteor. Soc.,* **113,** 899–927.

Sud, Y. C., and W. K.-M. Lau, 1996: Comments on ''Variability of summer rainfall over tropical North Africa (1906–92): Observation and modeling'' by Rowell, Folland, Maskell, and Ward (1995). *Quart. J. Roy. Meteor. Soc.,* **122,** 1001–1006.

Xue, Y., 1997: Biosphere feedback on regional climate in tropical North Africa. *Quart. J. Roy. Meteor. Soc.,* **123B,** 1483–1515.

——, and J. Shukla, 1993: The influence of land surface properties on Sahel climate. Part I: Desertification. *J. Climate,* **6,** 2232–2245.

——, and ——, 1996: The influence of land surface properties on Sahel climate. Part II: Afforestation. *J. Climate,* **9,** 3260–3275.

——, K. N. Liou, and A. Kasahara, 1990: Investigation of the biogeophysical feedback on the African climate using a two-dimensional model. *J. Climate,* **3,** 337–352.